Published by: ***Higher Institute of Engineering and Technology, Kafrelsheikh*** **(KFS-HIET)**

Journal homepage: https://jiet.journals.ekb.eg/

Print ISSN 3009-7207 **Online ISSN** 3009-7568

Finite Element Investigation of Space Trusses with Concrete-Filled Tubular Steel Members

*Mohamed I. Rady[1], Kamel S. Kandel[2], Maher M. Elabd[2]

[1]*Civil Engineering Department, Higher Institute of Engineering and Technology, Kafrelsheikh, Egypt*

[2]*Civil Engineering Department, Faculty of Engineering, Menoufia University, Shibin Elkom, Egypt*

Received: 28 January 2024; Revised: 3 May 2024; Accepted: 10 June 2024

ABSTRACT: Space trusses are three-dimensional structural systems which widely used in recent decades to cover large areas like halls, stadiums, and airports. The space trusses provided a lightweight and economical solution with fast construction. Traditional space trusses were made of hollow steel tube members that connected in joints of trusses. The paper presents a new composite technique to improve the behavior of space trusses. The hollow steel members were replaced with concrete-filled tubular steel members (CFST). The paper presents an investigation of Space Trusses with CFST Members through finite element modeling. The space trusses had a real scale with square dimensions of 20000 mm x 20000 mm. The paper presented parameters like truss member length and CFST member's location. The investigation presented results like ultimate load and cross-ponding central deflection. The investigation reported the replacement of hollow steel members with CFST elements in space trusses, led to an improvement in the behavior of space steel trusses.

KEYWORDS: Steel, concrete, space truss, concrete-filled tubular steel, and finite element.

1. INTRODUCTION

A space truss can be defined as a three-dimensional structural system assembled of linear elements. It is composed of two parallel grid layers of members interconnected by diagonal members, see Fig. 1. The space truss members were usually tubular sections. Tubular members were characterized by lightweight and high stiffness ratio. Previous studies investigated the behavior of space trusses and tried to improve their properties. The paper focuses on using the composite action method to improve the space truss behavior. Composite action is enhanced by using two materials as one to improve the overall behavior. Previous studies used a concrete slab deck connected to the upper layer of the space truss. Other studies selected sandwich panels over the space truss. In this study, as mentioned before, the use of CFST members improves the behavior of steel members subject to axial compression force, like upper chord and diagonal members. The hollow truss members will be replaced with CFST members. Tubular members were easy to fill with concrete which improved the behavior. FE programs provide to study of many parameters for research problems at a low cost. This leads to more information and knowledge compared to experimental investigation which is more expensive and complex with a narrow range of parameters and more fabrication and testing imperfections. So, the paper investigates that technique on space trusses with real scale using finite element modeling.

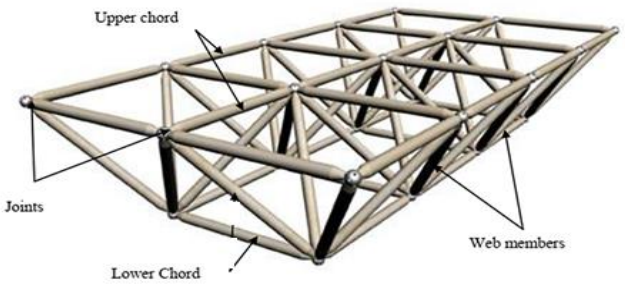

Fig. 1. Space Truss Components.

 *Corresponding author email: mohamedmousa@kfs-hiet.edu.eg

Studies [1&2] presented experimental tests on space trusses on a small scale. The space trusses had dimensions of 1830 mm in length and width, and height of 216 mm. The studies reported that the tested trusses showed linear behavior until the failure of the first few compression members, which occurred nearly at the same load level in all tests. Space truss had dimensions 4000 x 4000 mm with a depth of 575 mm investigated [3]. Space truss tested to failure under static load. The bottom cord and diagonal members had a pipe cross-section shape with an outer diameter of 28.53 mm and a wall thickness of 1.63 mm. The diagonal members at supports had a bigger section with a 60.3 mm outer diameter and a 3.2 mm wall thickness. The upper chord cross-section of the trusses was variable. The first truss had a channel 51 x 38 x 6.4 mm, while the other two space trusses had 40 x 24 x 1.6 mm.

Truss 3 was enhanced by a concrete slab connected to the upper chord to study the efficiency of composite action in improving the behavior of space trusses. The failure of the steel composite truss occurred suddenly and progressively. The failure shape was a buckling mode that started on the upper chord. The study reported the upper member's failure due to overall buckling. Investigation [4] presented the behavior of space trusses through experimental tests. They suggested using a fully scaled space truss with N-type segments. The model had a 3 × 3 lower layer grid and a 2 × 2 upper layer grid, and the theoretical length of the grid bars and diagonals was 1200 mm. The collapse was due to the local buckling of two opposite diagonals at the top center joint, where the load was applied. Three space trusses were made with different layout shapes with the same cross-section of members by [5].

The top chords were made of 13×13×1.8 mm square hollow section (SHS) steel tubes, while the web members were made of 13 × 2.0 mm circular hollow section (CHS) steel tubes; the bottom chords were made of 27 × 8.75 mm circular hollow section (CHS) steel tubes. As shown in Figure 2, the failure mode shape that occurred on the space truss after reaching the ultimate load was buckling in upper chord members. Investigation [6] studied the behavior of double-layer space trusses through a FE program. The results of the models were compared with previous experimental tests. The ABAQUS software program was used to model and discuss the behavior, carrying load capacity, and failure shape. The FE program included two space truss models with the same layout dimensions. The space truss had a square area of 1800 mm x 1800 mm with a height of 254.6 mm. The bottom-chord members were arranged in a 5x5 square grid, and the top chord members were in a 4x4 square grid.

Good agreement between the experimental and finite element results has been obtained. The proposed methods give a similar prediction of the space truss collapse process up to the point where it signifies the first failure in both models. The behavior of concrete-filled tubular steel members was investigated by [7], [8], and [9]. The studies presented the behavior of CFST and tubular members through experimental tests and FE modeling. Variables like specimen dimensions (cross-section and length) and concrete strengths were investigated. All columns were subjected to axial compression loading until failure. The cross-section of the column was square or rectangular. The dimension of square section column was 100x100x1.0 mm, 180x180x3.0 mm, and 280x280x2.0 mm with column length 300 mm, 540 mm, and 840 mm, respectively. The rectangular columns had a cross-section of 240x160x1.5 mm, 240x160x2.0 mm, and 240x160x3.0 mm with the same length 720 mm. The FE program included modeling of confined concrete, material modeling of high-strength stainless steel tubes, modeling of concrete-stainless steel tube interface, boundary conditions and load application, and finite element type and mesh. Study [10] investigated the load-carrying capacity and ductility of composite steel trusses compared to hollow steel trusses by studying the effect of using CFST truss members. The study included two experimental series. First, tests were conducted on CFST and hollow tube steel columns to measure the effect of the concrete used. Then, in the second series, trusses were made using the same tubes. The CFST columns had a square section SHS60x60x3 with a length of 2.00m and two boundary conditions were discussed: pin ends and fixed ends. The truss layout for experimental tests was a simply supported truss at end corners. From the experimental results: The maximum load resisted by the member in the composite truss was 29% higher than that of the steel truss. All steel and composite trusses had the same failure mode shape which was overall buckling of compression members, especially vertical members at loading cell and supports.

Study [11] investigated CFST trusses. The study included four circular hollow section tubular trusses that were multi-planar to ensure no lateral displacement occurred during testing. Only the top chords of trusses were infilled with concrete. The trusses had a span of 3000 mm with a height of 490 mm. Tubular trusses usually fail due to surface plasticity or punching shear of top chord members while concrete-filled multi-planar tubular trusses fail due to local buckling of straight brace members and surface plasticity of bottom chord members because top chord members are reinforced with in-filled concrete. Studies [12] and [13] presented an investigation into CFST trusses through FE study where finite element type, mesh size, and material modeling for steel tube and concrete infill were discussed. The validation of a FE was drawn using previous experimental study [11].

Also, load-carrying capacity and mode shape failure from finite element models were compared before extending parametric study with different spans and heights for CFST truss. Investigation [14, 15] presented an experimental FE program aimed at studying and investigating the behavior of CFST truss. Three trusses were tested with different parameters to measure the effect of composite action on truss behavior. Experimental trusses had the same general layout dimension with a span equal to 6000 mm divided into twelve panels and a height equal to 500 mm. Truss chords were circular hollow sections with diameter 100mm and thickness 4.9 mm while diagonal or braced members were circular hollow sections with diameter 57 mm and thickness 3.9 mm. The failure mode shape was cracking of bottom chord. Previous studies presented the space trusses through experimental tests, also on a small scale. In this paper, space trusses with real scale are modeled and studied using finite element investigation. The investigation included briefly the modeling steps.

2. Aim and Research Significance

The composite action technique was selected by using concrete-filled steel tube (CFST) members instead of traditional steel tubes. The CFST members had great compressive behavior, so the study replaced the steel members with high compression force with CFST members. This study aimed to use a finite element program to present and model space trusses with CFST members. Then validating the finite element models according to experimental samples. The validation of the finite element program was based on an experimental study drawn by [16]. Parametric study based on validation of FE program was drawn. Finally, presenting and discussing the results of parametric study.

3. Finite element modeling and validation

The current study presents an accurate finite element model for CFST and hollow tube steel members using the ABAQUS 2017 [17] software program. Finite Element Modeling included the identification of element part, mesh, and material properties as well as analysis type. Boundary conditions, contact between element parts, and load application were also included. Steel tubes were modeled as shell elements with reduced integration S4R while concrete-filled cores were modeled using 3-D solid C3D8. Hollow steel tube members were modeled as shell or wire elements. Several mesh sizes were tried to achieve reasonable mesh that provided reliable results while reducing computational time. It was found that a mesh size ratio of 1 (length): 1 (width): 2 (depth) for most elements achieved accurate results. The connection between the wire parts was simulated as a hinge which was created automatically. The option of coupling was selected for the connection between the shell or solid and wire parts. The meeting joint of parts was selected to create the coupling as the master constraint. Then select the shell or solid part surface as slave

3.1. Material Modeling of the Normal Confined Concrete and Steel Tube

To model the concrete core, a procedure similar to that presented by [7] was used. Fig. 2 illustrates the relationship between the equivalent uniaxial stress-strain curves for both unconfined and confined concrete. Where fc represents unconfined concrete cylinder compressive strength (equal to 0.8(fcu) where fcu is unconfined concrete cube compressive strength) while corresponding unconfined strain (εc) is taken as 0.003. From Equations 1 and 2, confined concrete compressive strength (fcc) and corresponding confined strain (εcc) can be determined respectively using equations proposed by Mander et al [18].

$$f_{cc} = f_c + k_1 f_1 \quad (1)$$

$$\varepsilon_{cc} = \varepsilon_c \left(1 + k_2 \frac{f_1}{f_c}\right) \quad (2)$$

$$E_{cc} = 4700\sqrt{f_{cc}} \ \text{MPa} \quad (3)$$

The stress-strain curve can also be distinguished in two parts (elastic part and plastic part). The linear part in the stress-strain curve of the normal concrete was defined by The ELASTIC option in ABAQUS. The elastic part properties are completely defined by giving the Young's modulus Ecc from equation 3 and the Poisson's ratio which was taken equal to 0.2. The plastic part of the concrete was modeled using the DRUCKER PRAGER model available in ABAQUS [17]. Two parameters (*DRUCKER PRAGER and *DRUCKER PRAGER HARDENING) were used to define the yield stage of confined concrete. The material angle of friction (b) and the ratio of flow stress in tri-axial tension to that in compression (K) were taken as 20° and 0.8 respectively, as recommended by Hu et al. [19].

For modeling steel material, elastic properties were completely defined by providing Young's modulus (E) and Poisson's ratio (ν), the values of 200000 MPa and 0.3; respectively. The nonlinear part of the steel material's stress-strain curve was modeled using the PLASTIC option available in ABAQUS [17] and [19]. Contact elements were used to model the interaction between the internal surface of the steel tube and the external surface of the concrete core. The coefficient of friction between two faces was taken as 0.25 for analysis. The interface element allows surfaces to separate under tensile force influence but prevents penetration through a hard contact interface.

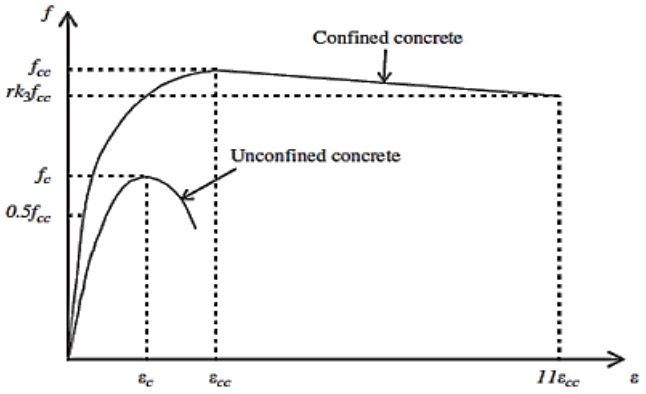

Fig. 2. Equivalent Uniaxial Stress-Strain Curves for Confined and Unconfined Concrete [18].

3.2. The finite Element Modeling Validation

A study [16] presented four space trusses tested under static load, which simply supported in four corners of space truss. Space trusses had length, and height equal to 3840 mm, 1280 mm, and 900 mm, respectively. Space truss members were made of circular hollow sections with the same length of 1000 mm. The space truss contains 3x1 panels. The panel had dimensions 1280 x 1280 mm members with an assure shape, see Fig. 3. Space trusses are made of circular hollow sections with cross-section dimensions shown in Table 1. The truss member dimension and cross section shown in fig. 4. The space trusses were two steel space trusses and two space trusses with CFST members. The CFST members are found in upper chords which are replaced with the hollow members in the steel trusses with the same cross-section of members. Also, the study presented a finite element modeling for the space trusses using the ABAQUS 2017[17] software program and compared the results of experimental tests and finite element modeling. Self-compacting concrete used with concrete strength 35 Mpa.

Table 1: Properties and Dimensions of Specimens of Space Truss Specimens by Mousa et al. [16]

Specimen Label	Truss Type	Upper Mesh Section	Lower Mesh & Diagonal Section	Upper Mesh Section				Lower Mesh & Diagonal Section			
				D (mm)	t (mm)	D/t	λ = Le / r	D (mm)	t (mm)	D/t	λ = Le / r
ST1	Steel	CHS42.0x3.0	CHS60.3x3.0	42.00	3.00	14.06	76.98	60.30	3.00	20.10	52.74
ST2		CHS48.8x2.8		48.80	2.80	17.14	66.83				
CT1	Composite	CHS42.0x3.0		42.00	3.00	14.06	76.98				
CT2		CHS48.8x2.8		48.80	2.80	17.14	66.83				

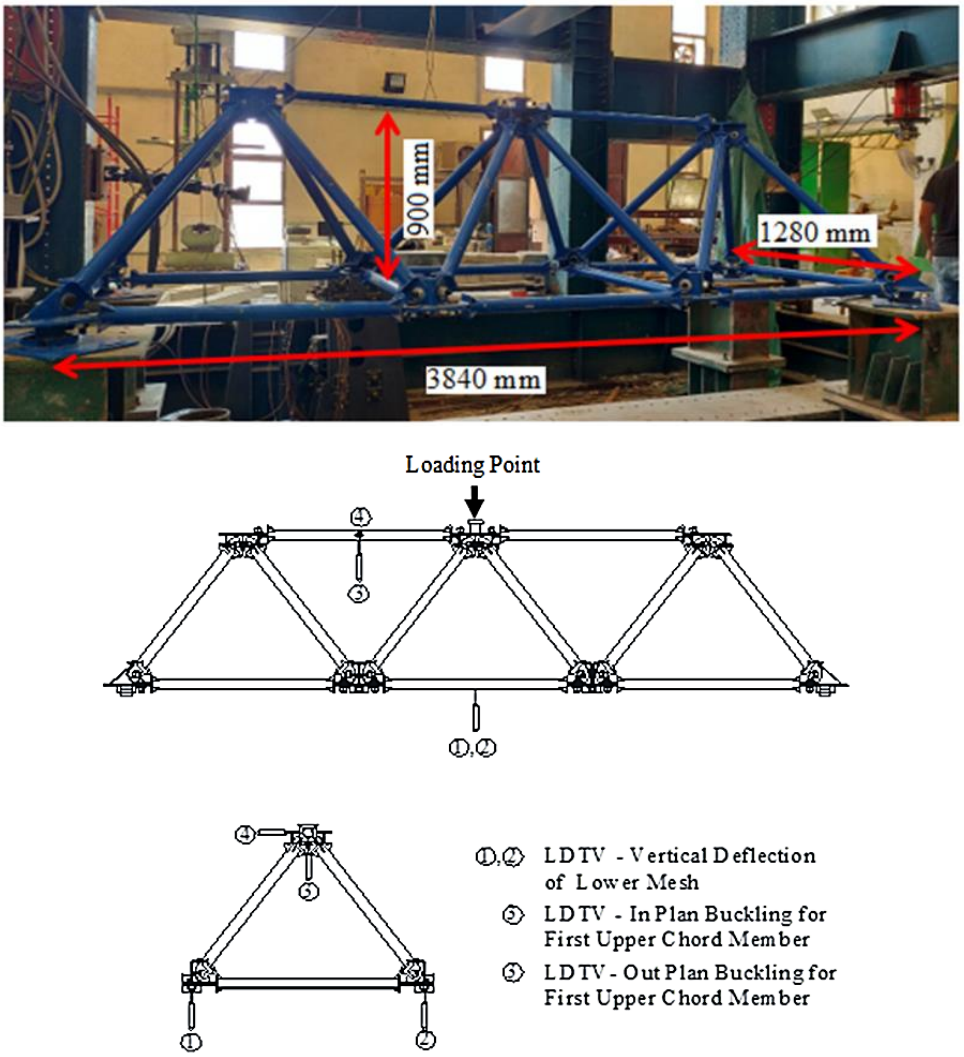

Fig. 3. Photo and Layout Dimension of Space Truss. [16]

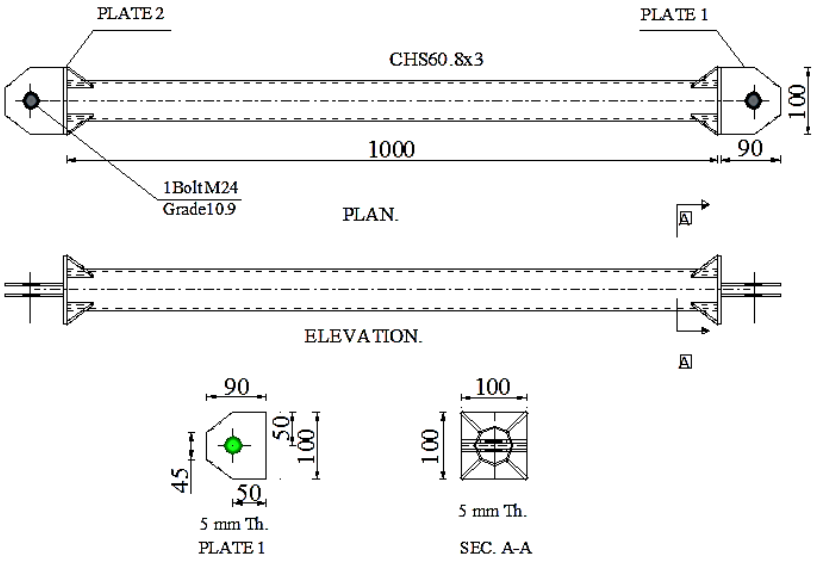

Fig. 4. Dimensions of Truss Members [16].

Table 2 presents comparison between results of experimental tests by authors (16) and FE models results for four space truss models. The mean difference ratio between experimental and FE results was 7.49%, with the highest and lowest values being 9.10% and 4.26% respectively.

Table 2: Experimental and FE Modeling Load Capacity of Space Truss Specimens [16].

Specimen Label	Truss Type	Upper Mesh Section	Lower Mesh & Diagonal Section	Fcu (MPa)	Fy (MPa)	PExp (kN)	PF.E. (kN)	Difference ratio %
ST1	Steel	CHS42.0x3.0	CHS60.3x3.0	------	295	132.87	141.13	6.22
ST2		CHS48.8x2.8		------	295	154.22	162.89	5.63
CT1	Composite	CHS42.0x3.0		35	295	145 .54	157.25	8.05
CT2		CHS48.8x2.8		35	295	186.25	202.56	8.76

Figs. 5 and 6 show the load-versus-mid span deflection findings from FE modeling and experimental testing on steel and composite space trusses, respectively. Generally, the FE modeling curves are separated into two sections. The first region begins at the start of the test and continues until the ultimate load is achieved. In this zone, load and deflection rise in tandem in a semi-linear fashion. The second zone extends from the ultimate load until the conclusion of testing when the load drops with a fast rise in deflection for CT1 and CT2. The curves from FE modeling and experimental tests were almost identical. However, deflection using finite element modeling was found to be lower than that achieved from experimental measurements.

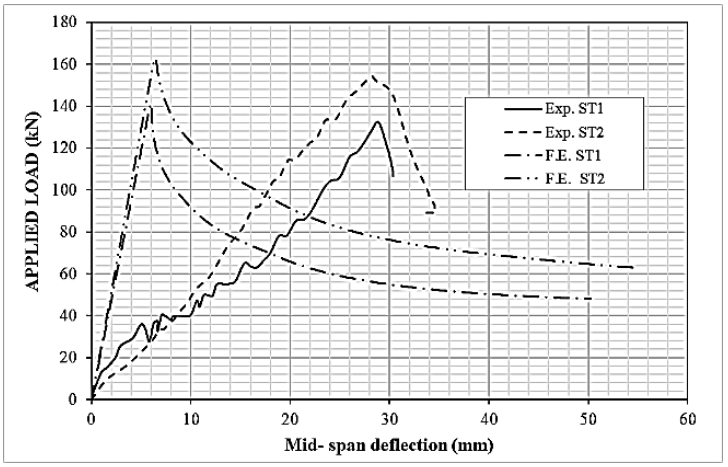

Fig. 5. Experimental and F.E. Modelling Load- Middle Span Deflection Curves for ST1 And ST2 [16].

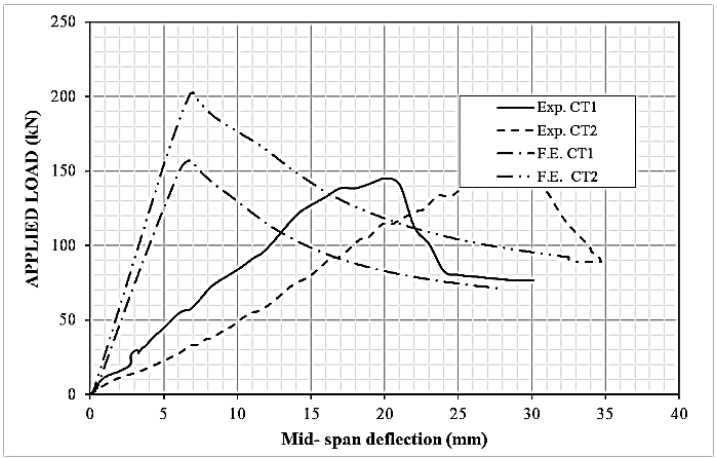

Fig. 6. Experimental and F.E. Modelling Load- Middle Span Deflection Curves for CT1 And CT2.

Figs. 7 to 10 demonstrate good agreement between failure mechanisms, ultimate load capacity, and deformations seen during experimental tests and FE analysis of space trusses ST1, ST2, and CT2. It should also be noted that compression failure in the upper chord component was the most common failure mode for all space trusses. The discussion indicates that there is good agreement between FE modeling and experimental test findings.

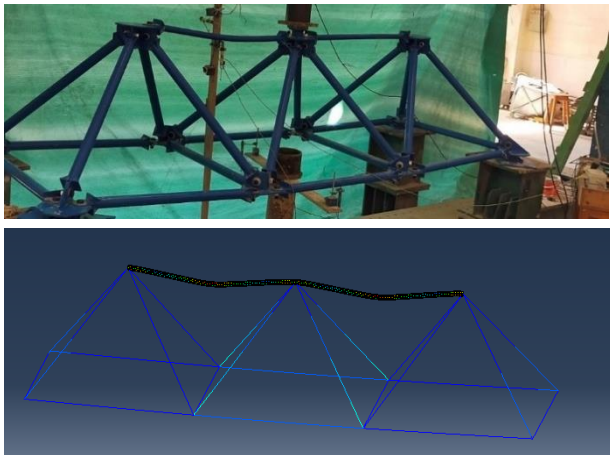

Fig. 7. F.E. Modelling and Experimental Deformed Shape of Steel Space Truss ST1.

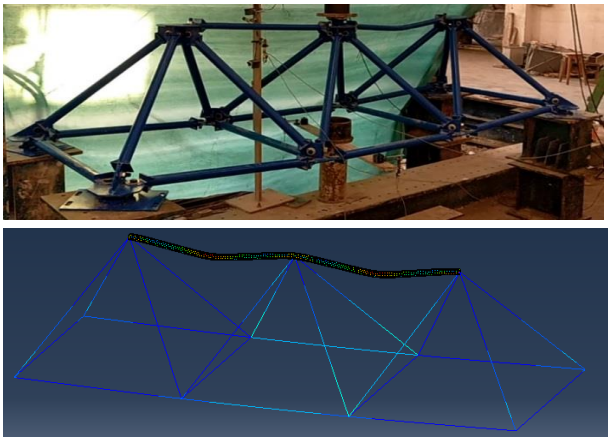

Fig. 8. F.E. Modelling and Experimental Deformed Shape of Steel Space Truss ST2.

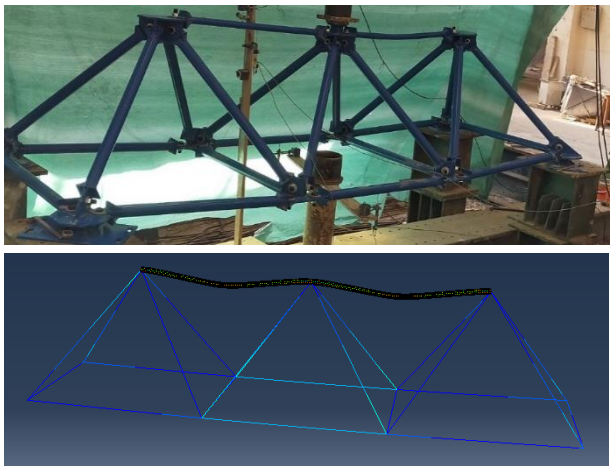

Fig. 9. F.E. Modelling and Experimental Deformed Shape of Steel Space Truss CT1.

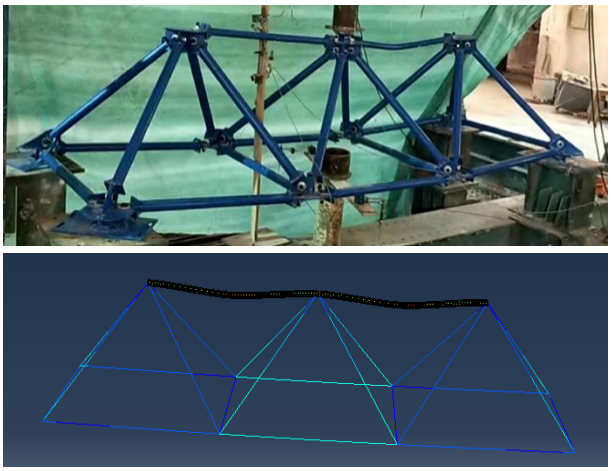

Fig. 10. F.E. Modelling and Experimental Deformed Shape of Steel Space Truss CT2.

4. PARAMETRIC STUDY

A fully scaled space truss with a span of 20000 x 20000 mm2 was selected for this study. The space truss was a square offset square type. The dimensions of the space trusses were fixed for all specimens so that we could compare the results of different parameters. The space trusses had four-corner support boundary conditions, see Fig. 11. Two different

member lengths were 1000 mm and 1250 mm. For space trusses with a member length of 1000 mm, the upper mesh consisted of 20 x 20 panels and had a height of 770 mm, while the lower mesh consisted of 19 x 19 panels. For a member length of 1250 mm, the space trusses had a height of 850 mm, with the upper mesh consisting of 16 x 16 panels and the lower mesh consisting of 15 x 15 panels. The space trusses were a circular hollow section with a diameter of 42.40 mm and a thickness of 3.00 mm for the upper mesh and diagonal members, while the lower mesh was a circular hollow section with a diameter of 60.30 mm and a thickness of 5.00 mm.

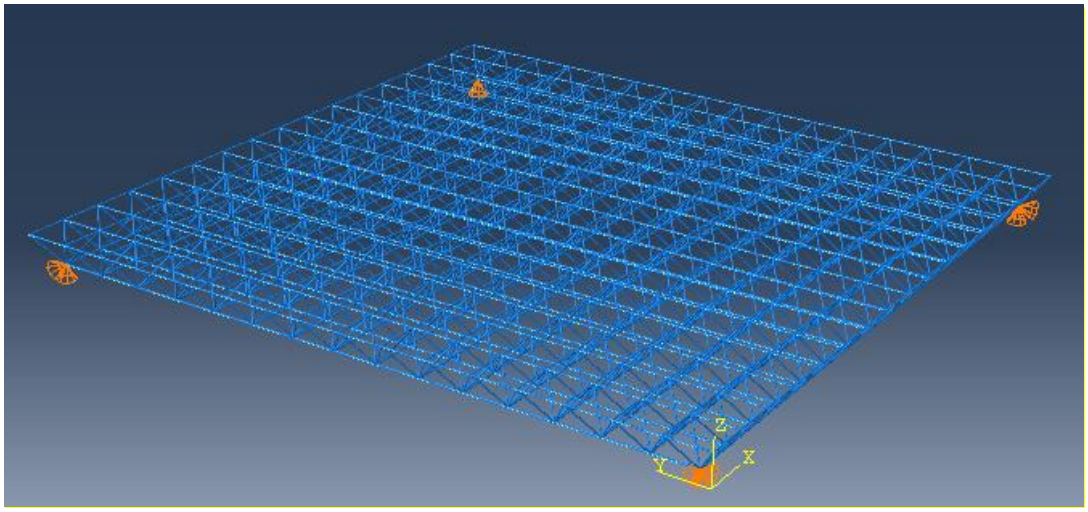

Fig. 11. Boundary Condition of Space Trusses Specimens.

It is known that concrete-filled tubular members have great efficiency in carrying axial compression forces. Thus, circular hollow steel members with high axial compression force were filled with concrete-filled tubular members. It was noted that the upper mesh had compression axial force. So, the last parameter is replacing the tubular steel members in the upper mesh with CFST members. The outer rings of rows had larger axial forces than the inner rings. Therefore, the parameter was the location of concrete-filled tubular steel members. Five variables were studied for the boundary condition case, see Fig. 12.

1- Steel space truss.

2. Composite space truss with CFST members in two outer rows of the upper mesh,

3. Composite space truss with CFST members in four outer rows of the upper mesh,

4. Composite space truss with CFST members in all upper mesh and

5. Composite space truss with X-shaped CFST members in the upper mesh.

Four corners of the lower mesh were selected with the minimum reaction for stability of trusses, and all rotations of supports were allowed. The first support prevented all displacement (X, Y, and Z) axes, the second support prevented displacement for X and Z axes, the third support prevented displacement for Y and Z axes, and the fourth support prevented displacement for the Z axis only. All truss specimens were subjected to a service load applied to all joints of the upper mesh. The intermediate joint was subject to a load value of P, the edge joint was subject to a load value of 0.5P, and the corner joint was subject to a load value of 0.25P.

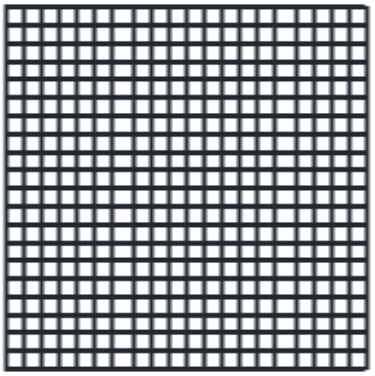

1- Steel Space Truss

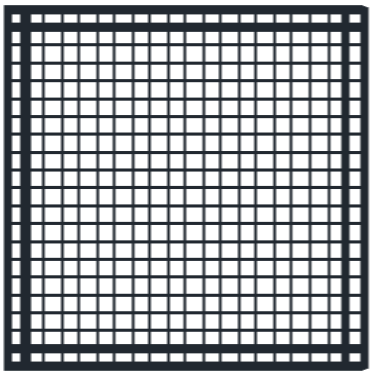

2- CFST Members in Two Outer Rings

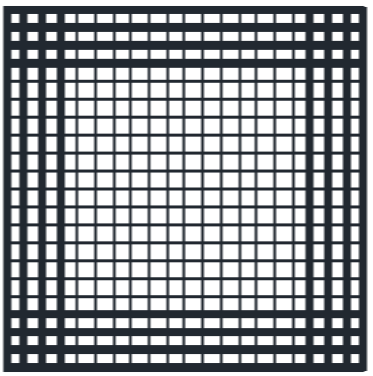

3- CFST Members in Four Outer Rings

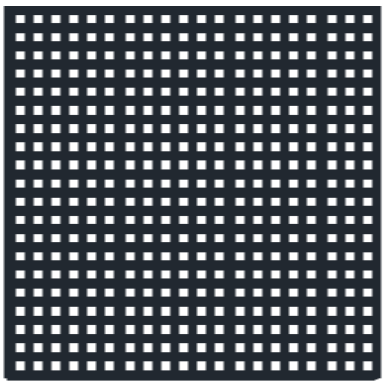

4- CFST Members in All Upper Mesh

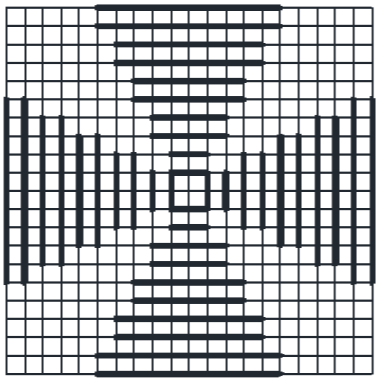

5- X- Shape CFST Members in Upper Mesh

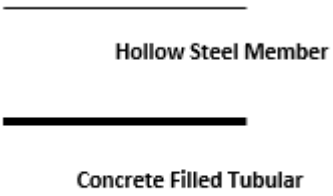

Fig. 12. Arrangement of Upper Mesh Members for Space Truss.

The parametric study contains 10 space trusses; 2 hollow tubular steel space trusses and 8 steel space trusses with CFST members. Specimens are divided into two groups according to the length of space truss members. The first group had a member length of 1000 mm and was labeled T1. The second group had a member length of 1250 mm and was labeled T2. Each space truss had a label indicating its properties. Steel trusses were labeled with "S" and composite trusses with "C". Each group contained one steel space truss and four composite space trusses. Composite trusses were labeled "2R", "4R", "AR", or "X" according to the location of CFST members on the upper mesh, see Table 3.

Table 3: Properties and Dimensions of Specimens.

Group	Specimen Label	Member cross-section		Concrete Strength Fcu (MPa)	Steel Strength Fy (MPa)	CFST Members
		Upper mesh & Diagonal	Lower mesh			
Group 1	ST1	CHS42.40x3.00	CHS60.30x5.00	----	295	N.A.
	CT1-2R			35	295	Outer two ring
	CT1-4R			35	295	Outer four ring
	CT1-AR			35	295	All upper mesh
	CT1-X			35	295	X-shape on the upper mesh
Group 2	ST2	CHS42.40x3.00	CHS60.0x5.00	----	295	N.A.
	CT2-2R			35	295	Outer two ring
	CT2-4R			35	295	Outer four ring
	CT2-AR			35	295	All upper mesh
	CT2-X			35	295	X-shape on the upper mesh

5. Results and Discussion of Parametric Study

Two main results were discussed to measure the effect of using the CFST members instead of tubular members: ultimate load capacity and cross-ponding central deflection as shown in Table 4. Also, table 4 presents the ratio of increase in ultimate load capacity. Fig. 13 presented compression between the ultimate load capacities between all specimens. As shown in Table 4, the ultimate load capacity was improved using CFST members. The best ratio of increase was recorded with truss CT1-AR with a value of 10.45%. Truss CT1-X had a ratio of increase of 9.06%, which is near to truss CT1-4R. From an economic perspective, truss CT1-X is the better composite truss with CFST members in an X-shape in the upper mesh. The percentage of CFST members to upper chord members for truss CT1-X is 28%, while truss CT1-AR had CFST members in all upper mesh. The percentage of CFST members to upper mesh members is 19% and 38% for CT1-2R and CT1-4R, respectively. Steel space truss ST2 recorded an ultimate load of 1.54 kN. Space truss CT2-2R, which contains CFST members in the outer two rings of the upper mesh, had a predicted ultimate load of 1.66 kN with a ratio increase of 7.87%. Space truss CT2-4R, which contains CFST members in the outer four rings of the upper mesh, had a predicted ultimate load of 1.69 kN with a ratio of increase of 9.71%.

Table 4: Ultimate Load and Maximum Central Deflection of Specimens.

Group	Specimen Label	Member cross-section		CFST Members	Ultimate Load P (kN)	Central Deflection δ (mm)	Ratio of Increase Pc /Ps (%)
		Upper mesh & Diagonal	Lower mesh				
Group 1	ST1	CHS42.40x3.00	CHS60.30x5.00	N.A.	1.03	137.31	----
	CT1-2R			Outer two ring	1.08	138.85	5.20
	CT1-4R			Outer four ring	1.11	139.89	7.72
	CT1-AR			All upper mesh	1.14	142.68	10.45
	CT1-X			X-shape on the upper mesh	1.12	142.58	9.06
Group 2	ST2	CHS42.40x3.00	CHS60.0x5.00	N.A.	1.54	113.22	----
	CT2-2R			Outer two ring	1.66	116.61	7.87
	CT2-4R			Outer four ring	1.69	118.88	9.71
	CT2-AR			All upper mesh	1.72	121.14	11.66
	CT2-X			X-shape on the upper mesh	1.71	120.01	11.01

Space truss CT2-AR, which contains CFST members in all members of the upper mesh, had a predicted ultimate load of 1.72 kN with a ratio of increase of 11.66%. Space truss CT2-X, which contains CFST members in an X-shape in the upper mesh, had a predicted ultimate load of 1.71 kN with a ratio of increase of 11.00%.

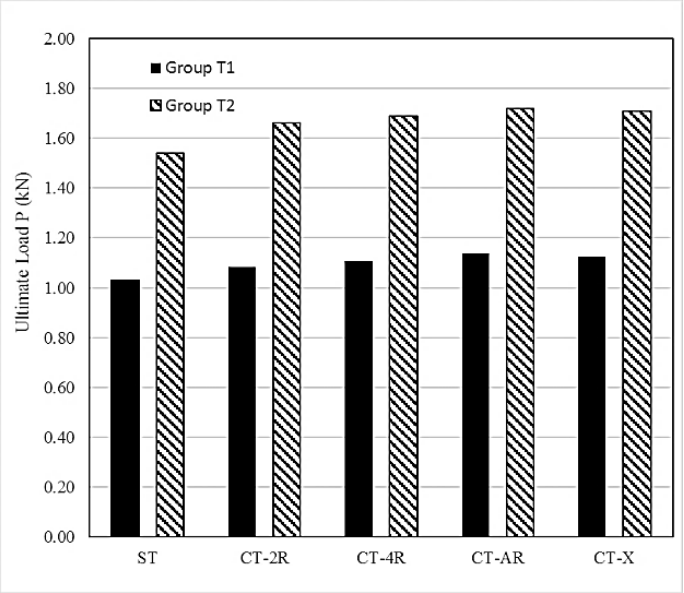

Fig. 13. Ultimate Load of Space Trusses specimens.

The ultimate load against central deflection relations for space truss specimens are presented in Figs. 14 and 15. The relations started linearly and then converted to nonlinear at failure load before the space trusses collapsed at ultimate load. This means that all space trusses failed due to compression in upper mesh members as shown in figs. 16 to 25 which previewed the deformed shape of space trusses.

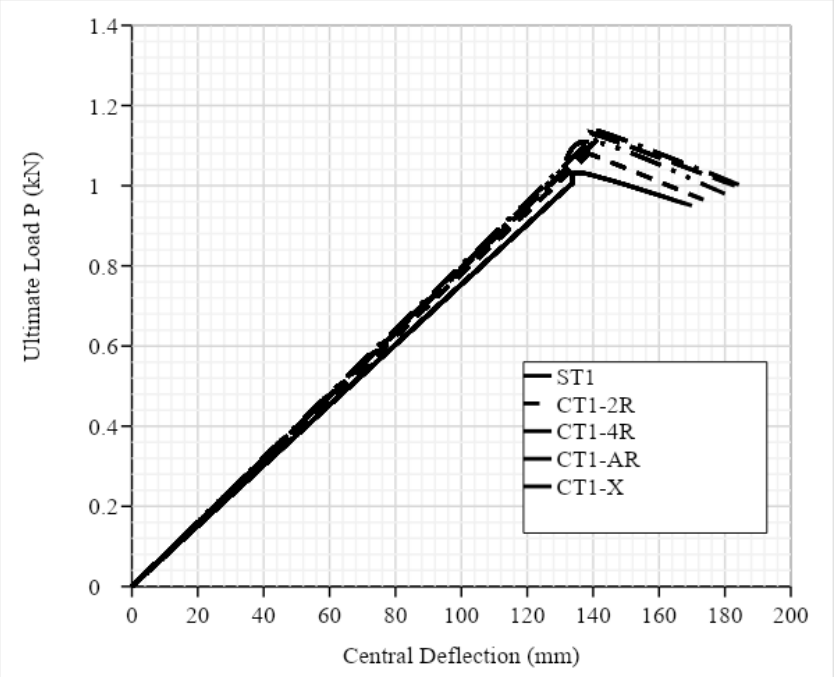

Fig. 14. Relation of Ultimate Load and Central Deflection for Space Trusses ST1, CT1-2R, CT1-4R, CT1-AR and CT1-X.

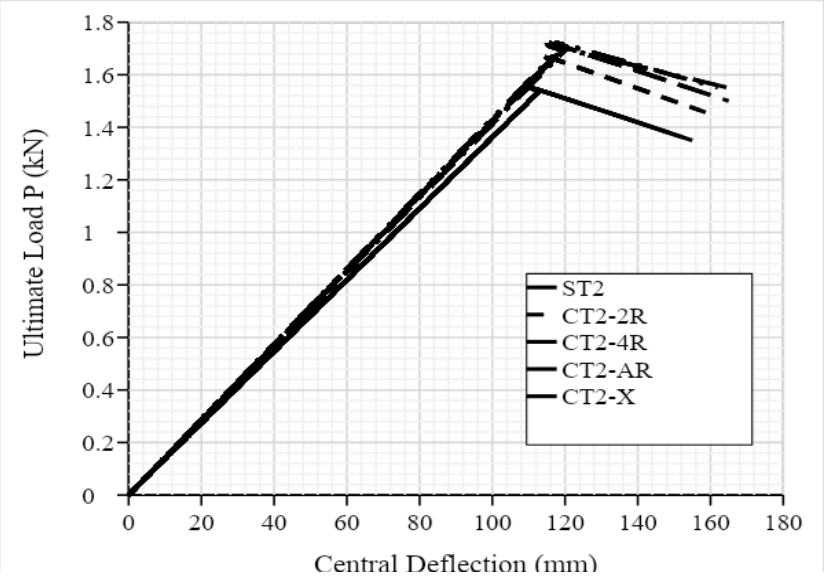

Fig. 15. Relation of Ultimate Load and Central Deflection for Space Trusses ST2, CT2-2R, CT2-4R, CT2-AR and CT2-X.

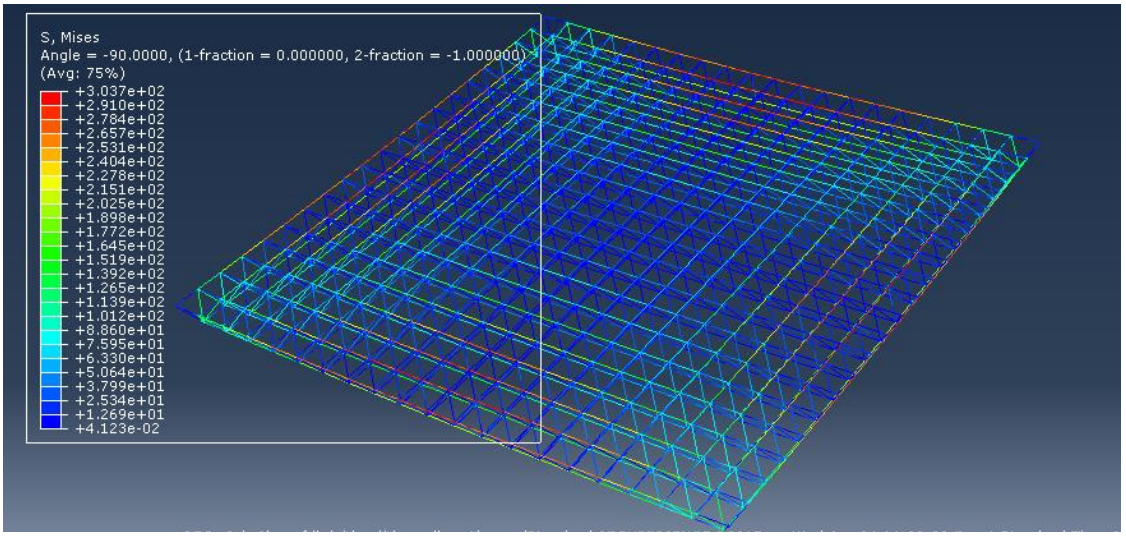

Fig. 16. F.E. Modelling Deformed Shape of Space Truss ST1.

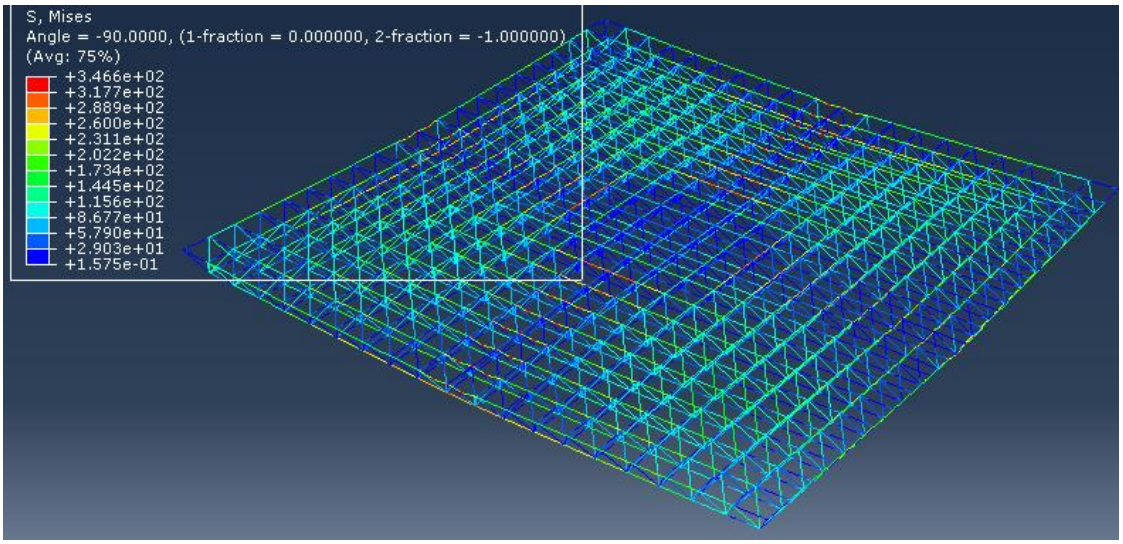

Fig. 17. F.E. Modelling Deformed Shape of Space Truss CT1-2R.

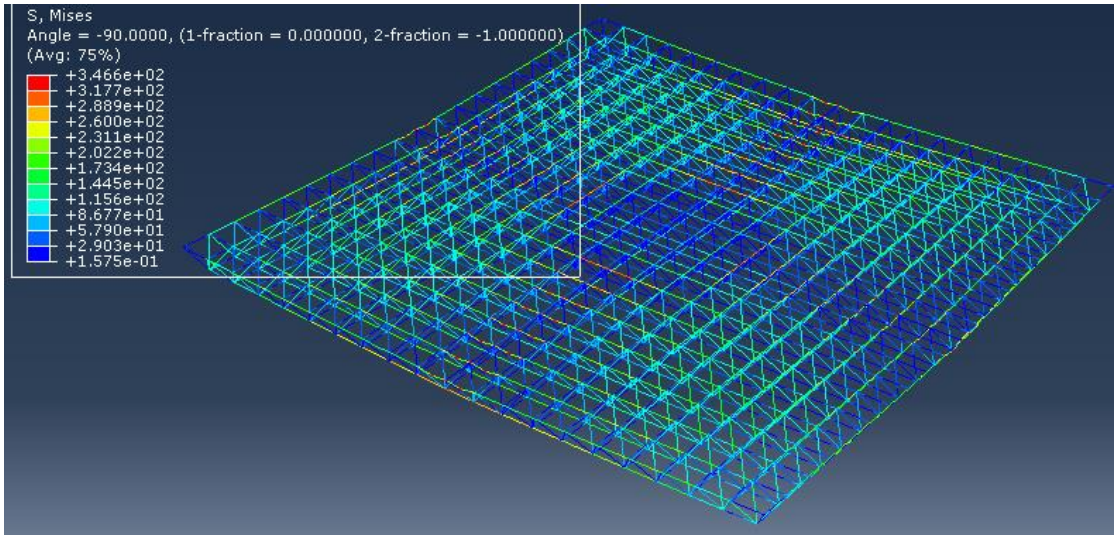

Fig. 18. F.E. F.E. Modelling Deformed Shape of Space Truss CT1-4R.

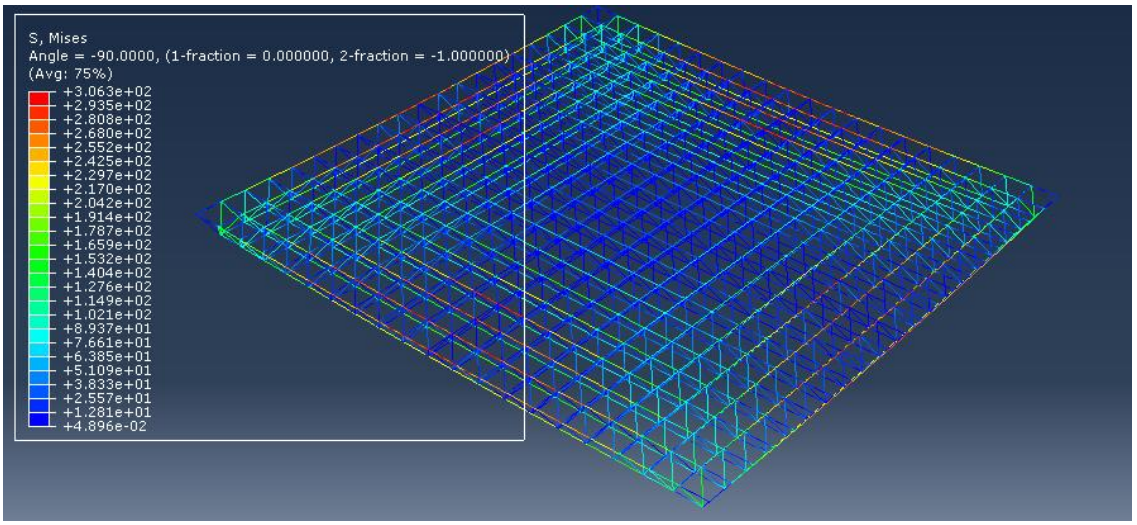

Fig. 19. F.E. Modelling Deformed Shape of Space Truss CT1-AR..

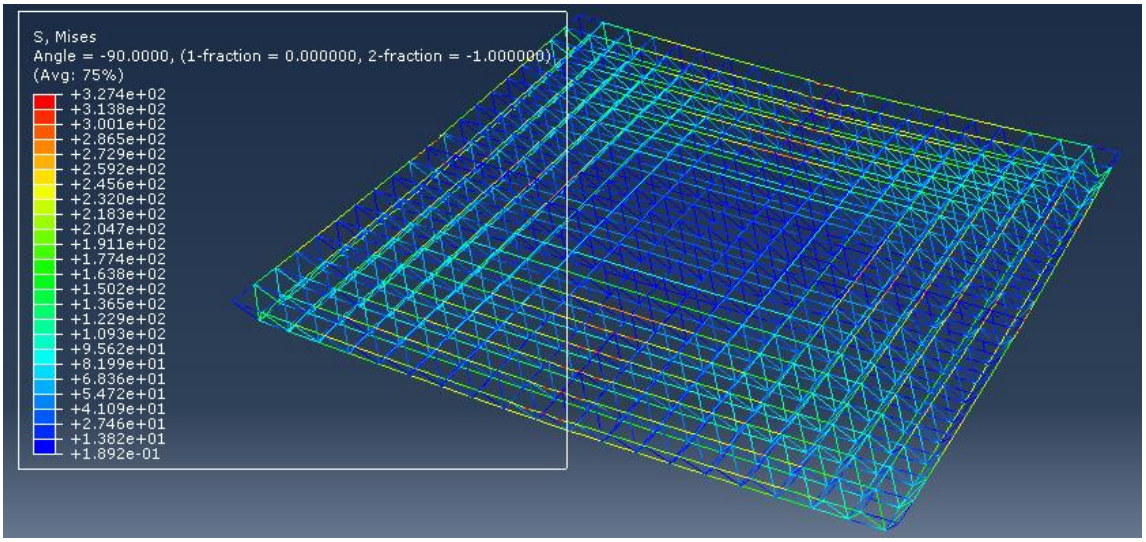

Fig. 20. F.E. Modelling Deformed Shape of Space Truss CT1-X.

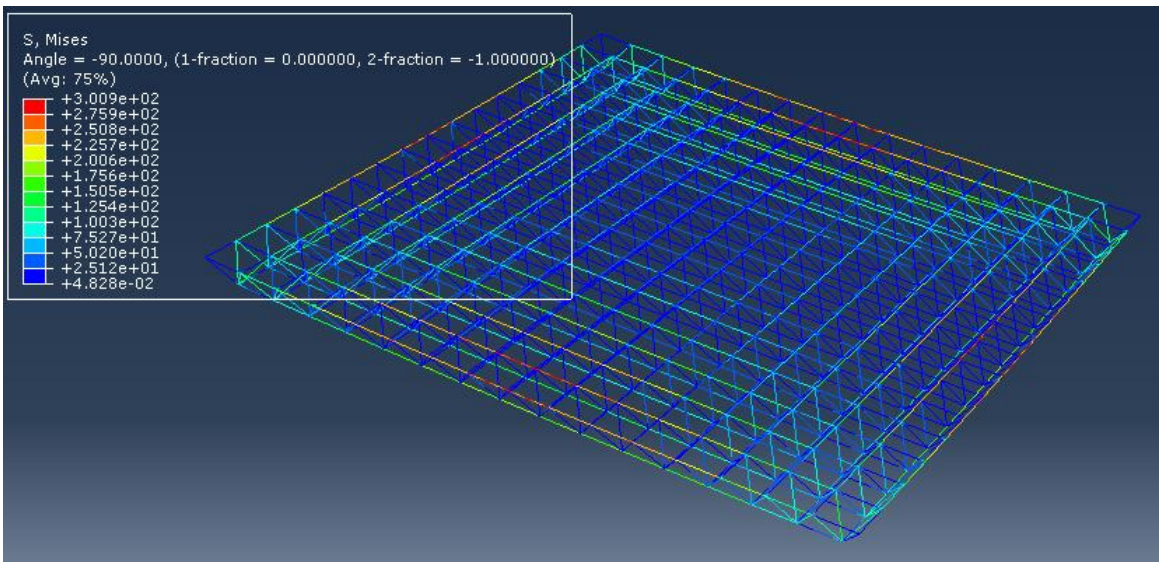

Fig. 21. F.E. Modelling Deformed Shape of Space Truss ST2.

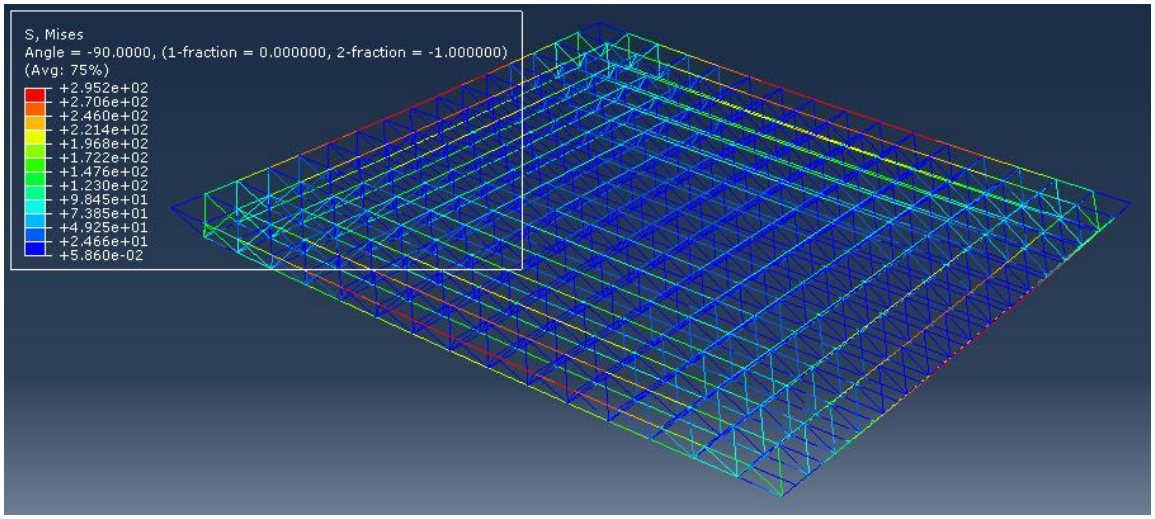

Fig. 22. F.E. Modelling Deformed Shape of Space Truss CT2-2R.

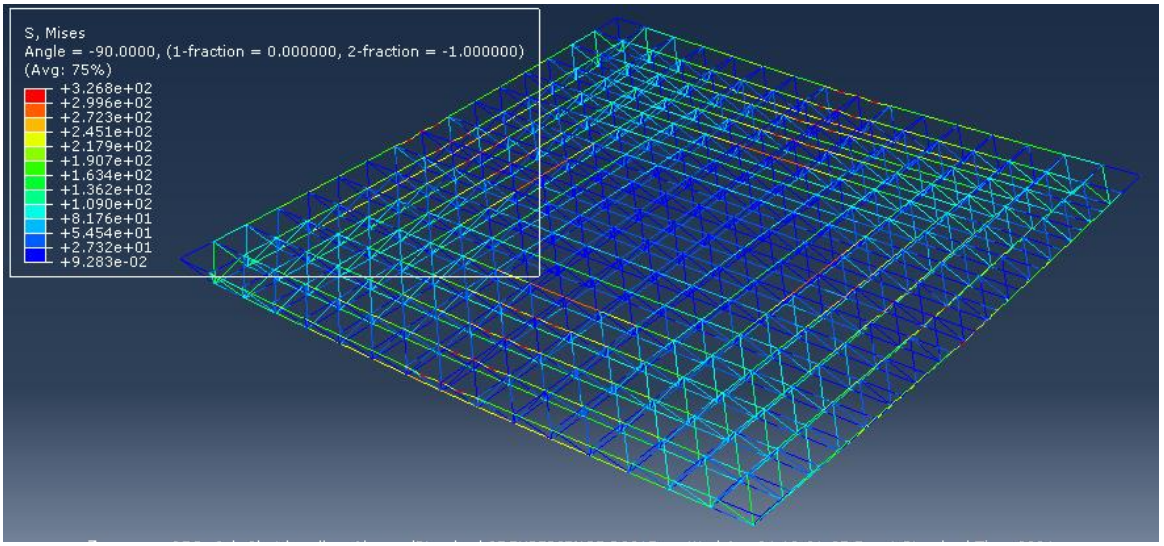

Fig. 23. F.E. Modelling Deformed Shape of Space Truss CT2-4R.

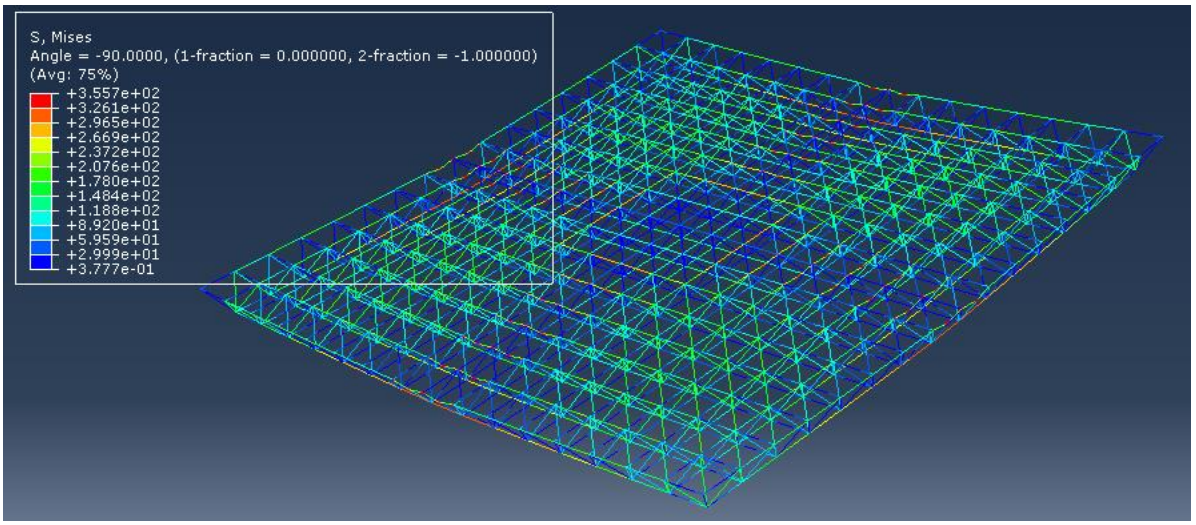

Fig. 24. F.E. Modelling Deformed Shape of Space Truss CT2-AR.

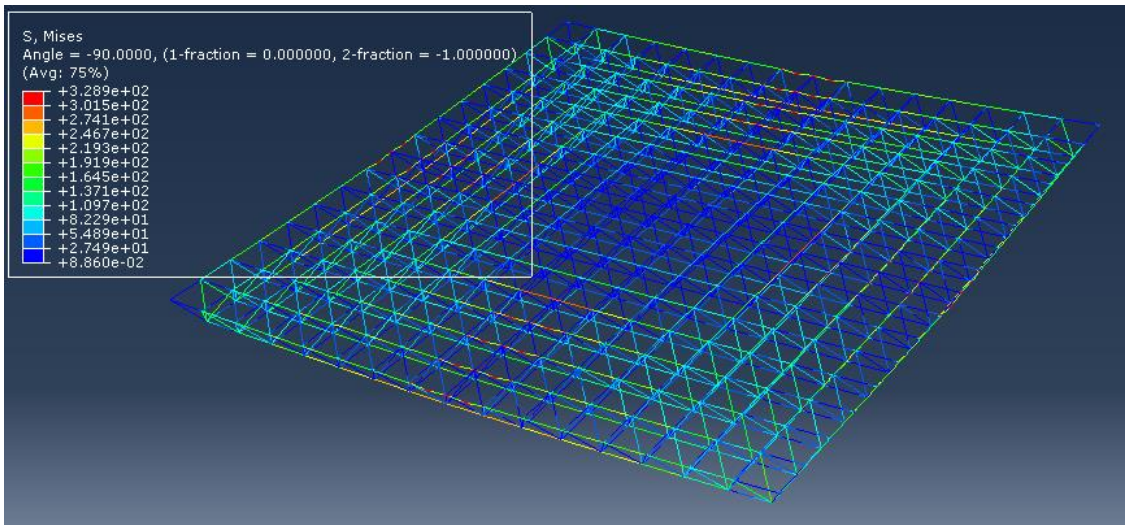

Fig. 25. F.E. Modelling Deformed Shape of Space Truss CT2-X.

6. CONCLUSIONS

The study previewed finite element modeling investigation for space trusses with CFST members. The study presents parameters like member length and location of CFST members. Also, the effect of using the composite action of the CFST replacing technique is presented. The following conclusions can be drawn from the results:

1- Filling steel tubes with concrete to form CFST members led to enhancements in the behavior of compression members compared to hollow tubular steel members in terms of ultimate load capacity.

2- The most highly loaded compression elements were located at the first two rows of the outer edges, so the use of CFST was recommended for these elements.

3- For CFST member location parameter, each variable had a CFST member to steel member ratio for the upper mesh of 19%, 38%, 100%, and 28% for CT-2R, CT-4R, CT-AR, and CT-X space trusses respectively. The CT-AR composite space truss had the greatest ratio of increase in ultimate load. The optimum economic space truss was determined to be the CT-X composite space truss with a CFST member to upper mesh member ratio of 28%.

4- All space trusses failed by global buckling due to compression in upper mesh members.

REFERENCES

[1] L. C. Schmidt, P. R. Morgan, and L. K. Stevens, "The influence of imperfections on the behavior of a space truss", Second International Conference on Space Structures, University of Surrey, Billing & Sons Limited, UK, September 1975: pp 55-64, 1975.

[2] L. C. Schmidt, "Member buckling characteristics and space truss behavior", lASS World Congress on Space Enclosures, Building Research Centre, Concordia University Montreal, July 1976: pp 849-857, 1975

[3] A. I. El-Sheikh and R. E. McConnel, "Experimental study of behavior of composite space trusses," J. Struct. Eng. (United States), vol. 119, no. 3, pp. 747–766, 1993, doi: 10.1061/(ASCE)0733-9445(1993)119:3(747).

[4] A. Fülöp and M. Iványi, "Experimentally analyzed stability and ductility behaviour of a space-truss roof system," Thin-Walled Struct., vol. 42, no. 2, pp. 309–320, 2004, doi: 10.1016/S0263-8231(03)00062-4.

[5] J. W. Kim, J. J. Kim, and H. J. Rhew, "Analysis and experiment for the formation and ultimate load testing of a hypar space truss," J. Constr. Steel Res., vol. 62, no. 1–2, pp. 189–193, 2006, doi: 10.1016/j.jcsr.2005.04.020.

[6] Y. Sahol Hamid, P. Disney, and G. A. R. Parke, "Progressive Collapse of Double Layer Space Trusses," Iabse-Iass Symp. London 2011, no. August 2011, 2015, doi: 10.13140/2.1.4215.2328.

[7] B. Young and E. Ellobody, "Experimental investigation of concrete-filled cold-formed high strength stainless steel tube columns," J. Constr. Steel Res., vol. 62, no. 5, pp. 484–492, 2006, doi: 10.1016/j.jcsr.2005.08.004.

[8] E. Ellobody, "Nonlinear behavior of concrete-filled stainless steel stiffened slender tube columns," Thin-Walled Struct., vol. 45, no. 3, pp. 259–273, 2007, doi: 10.1016/j.tws.2007.02.011.

[9] E. Ellobody, "Numerical modelling of fibre reinforced concrete-filled stainless steel tubular columns," Thin-Walled

Struct., vol. 63, pp. 1–12, 2013, doi: 10.1016/j.tws.2012.10.005.

[10] B. Uy, Z. Tao, and L. H. Han, "Behaviour of short and slender concrete-filled stainless steel tubular columns," J. Constr. Steel Res., vol. 67, no. 3, pp. 360–378, 2011, doi: 10.1016/j.jcsr.2010.10.004.

[11] M. Dundu, "Column buckling tests of hot-rolled concrete filled square hollow sections of mild to high strength steel," Eng. Struct., vol. 127, pp. 73–85, 2016, doi: 10.1016/j.engstruct.2016.08.039.

[12] Y. Chen, R. Feng, and S. Gao, "Experimental study of concrete-filled multiplanar circular hollow section tubular trusses," Thin-Walled Struct., vol. 94, pp. 199–213, 2015, doi: 10.1016/j.tws.2015.04.013.

[13] L. H. Han, W. Xu, S. H. He, and Z. Tao, "Flexural behaviour of concrete filled steel tubular (CFST) chord to hollow tubular brace truss: Experiments," J. Constr. Steel Res., vol. 109, pp. 137–151, 2015, doi: 10.1016/j.jcsr.2015.03.002.

[14] Y. H. Huang, A. R. Liu, J. Y. Fu, and Y. L. Pi, "Experimental investigation of the flexural behavior of CFST trusses with interfacial imperfection," J. Constr. Steel Res., vol. 137, no. June, pp. 52–65, 2017, doi: 10.1016/j.jcsr.2017.06.009.

[15] W. Huang, L. Fenu, B. Chen, and B. Briseghella, "Experimental study on joint resistance and failure modes of concrete filled steel tubular (CFST) truss girders," J. Constr. Steel Res., vol. 141, pp. 241–250, 2018, doi: 10.1016/j.jcsr.2017.10.020.

[16] Mousa, mohamed, Kandeel, K., & Elabd, M. (2023). Behavior of Space Trusses With Cfst As Compression Elements1. ERJ. Engineering Research Journal, 0(0), 0–0. https://doi.org/10.21608/erjm.2023.204787.1257

[17] ABAQUS Standard Us r's Manual 004 , Vol. 1 –3. Version 6.4. USA: Hibbitt, Karlsson and Sorensen Inc.

[18] Mander JB, Priestley MJN, Park R. (1988), "Theoretical stress–strain model for confined concrete", Journal of Structural Engineering, ASCE, Vol. 114, No. 8, pp. 1804–1826.

[19] Hu, H. ., S no ri W.C., "Constitutiv Mod ling of Con r t y Using Nonasso iat d Plasti ity", Journal of Materials in Civil Engineering , Vol. 1, No. 4, pp. 199 216, (1989).